A THESIS FOR THE DEGREE OF MASTER OF SCIENCE

Analyses of canopy light interception and photosynthesis of greenhouse tomato plants under diffuse films by using 3D plant model and ray-tracing simulation

3 차원 식물 모델과 광추적 시뮬레이션을 이용한 산란필름 하에서의 온실 토마토의 수광 및 광합성 분석

BY

JI YONG SHIN

FEBRUARY, 2020

MAJOR IN HORTICULTURAL SCIENCE AND
BIOTECHNOLOGY
DEPARTMENT OF PLANT SCIENCE
GRADUATE SCHOOL
COLLEGE OF AGRICULTURE AND LIFE SCIENCES
SEOUL NATIONAL UNIVERSITY

Analyses of canopy light interception and photosynthesis of greenhouse tomato plants under diffuse films by using 3D plant model and ray-tracing simulation

UNDER THE DIRECTION OF DR. JUNG EEK SON
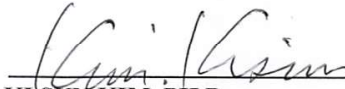SUBMITTED TO THE FACULTY OF THE GRADUATE SCHOOL OF
SEOUL NATIONAL UNIVERSITY

BY

JI YONG SHIN

DEPARTMENT OF PLANT SCIENCE
COLLEGE OF AGRICULTURE AND LIFE SCIENCES
SEOUL NATIONAL UNIVERSITY

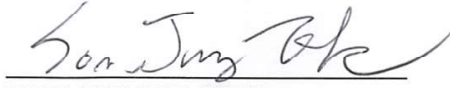FEBRUARY, 2020

APPROVED AS A QUALIFIED THESIS OF JI YONG SHIN
FOR THE DEGREE OF MASTER OF SCIENCE
BY THE COMMITTEE MEMBERS

CHAIRMAN: _____
KI SUN KIM, PH.D

VICE-CHAIRMAN: _____
JUNG EEK SON, PH.D

MEMBER: _____
CHANGHOO CHUN, PH.D

Analyses of canopy light interception and photosynthesis of greenhouse tomato plants under diffuse films by using 3D plant model and ray-tracing simulation

Ji Yong Shin

Department of Plant Science, Graduate School of Seoul National University

ABSTRACT

Recently diffuse covering materials have been used for increasing light use efficiency (LUE) through light distribution improvement. Although mathematical models and actual measurements have been tried to evaluate their effects, but these methods have disadvantages that cannot accurately measure the light distributions on plants and are only available under limited environmental conditions. The objective of this study was to quantitatively evaluate the effect of diffuse films on light interception and photosynthetic rate of tomato plants under various environmental conditions by using 3D-scanned plant models and optical simulation. To evaluate the reliability of ray-tracing simulation, measured light intensities by using 15 quantum sensors (5 horizontal x 3 vertical position) and estimated ones were compared in greenhouses covered with clear and diffuse films. In addition, light distributions were estimated and subsequently photosynthetic rates were calculated for two

main seasons of tomato harvest in Korea, summer and winter. Simulated light intensities showed good agreements with the measured ones with R^2 of 0.954 and 0.937 in the greenhouses covered with clear and diffuse films, respectively. In summer, when the external diffuse ratio was high, canopy photosynthetic rate and LUE did not tend to change with increasing haze factor. On the other hand, in winter, when external diffuse ratio was low, canopy photosynthetic rate and LUE increased up to 1.8% and 3.9%, respectively, but there was no significant difference. This method can be used not only to quantify canopy light interception and photosynthetic rate under various diffuse films, but also to select optimum diffuse films for various regions.

Additional key words: Monte Carlo method, scattered light, sun light, 3D scan, diffuse light ratio

CONTENTS

LIST OF TABLES

LIST OF FIGURES

LIST OF APPENDICES

INTRODUCTION

The amount of sunlight entering into greenhouses depends on the location and direction of the greenhouses. Even with the same amount of sunlight, the light use efficiency can be changed by light distribution inside the greenhouses and affects the plant growth and yield (Gonzalez-Real et al., 2007; Niinemets, 2007; Sarlikioti et al., 2011a).

The directional composition of the sunlight plays a pivotal role in the light distribution inside greenhouses (Gourdriaan and Van Larr, 1994). Sunlight is composed of direct and diffuse lights, which arrives in a straight line from the sun and in various directions, respectively. Under the diffuse light, light distribution on plants tends to be homogeneous (Farquhar and Roderick, 2003). The combined effect of light distribution and non-linear light saturation response of photosynthesis increases the canopy light use efficiency (Hollinger et al., 1994; Choudbury, 2001; Gu et al., 2002) and subsequently the plant growth (Hemming et al., 2007; Li et al., 2014a, b).

To take advantage of the diffuse light in greenhouse crop production, diffuse covering materials such as diffuse film and glass which increase the diffuseness of light without reducing light transmission have been used (Hemming et al., 2007; 2008; 2014). Under the diffuse covering materials, the vertical and horizontal light profiles of canopy become homogeneous (Li et al.,

2014a), and the crop growth and yield also increased (Hemming et al., 2007; Li et al., 2014a, b).

For evaluating the effect of diffuse light on plants, estimation with mathematical models and actual measurement with quantum sensors have been conducted (Gu et al., 2002; Farquhar and Roderick, 2003; Li et al., 2014a). However, despite being powerful tools, existing mathematical models have important constraints that only predict the average light intensity of non-uniform light distribution (Norman, 1980; dePury and Farquhar, 1997), resulting in the decrease of model robustness (Zhu et al., 2012). Actual measurements considering heterogeneity also have limitations that sensors can only be installed at empty spaces inside the canopy, not at exact positions near plants. Therefore, the light interception by plant surface cannot be measured. In addition, measurements with sensors only can be done in certain conditions that crops are actually being grown. Thus, even though the effect of diffuse covering material can be greatly changed by location and season (Li and Yang, 2015), only limited ranges of evaluation could be conducted.

Recently, many researchers have estimated light distributions on plant canopy (Buck-Sorlin et al., 2011; Sievänen et al., 2014; Henke and Buck-Sorlin, 2018), and photosynthesis combining canopy photosynthesis model (Buck-Sorlin et al., 2011; Sarlikioti et al., 2011a; de Visser et al., 2014; Kim et al., 2016; Jung et al., 2018) by using 3D plant models and ray-tracing simulation. Through this method, the heterogeneities in spatial light

distribution, estimation of light interception on plant surface, and implementation of various environmental conditions could be considered. In addition, elaborate 3D plant models have become available through high resolution 3D-scanning and process technologies (Burgess et al., 2017; Townsend et al., 2018).

The objective of this study was to quantitatively evaluate the effect of diffuse films on light interception and photosynthetic rate of tomato plants under various environmental conditions by using 3D-scanned plant models and optical simulation.

LITERATURE REVIEW

Diffuse Light and Diffuse Films

Sun light is composed of diffuse and direct lights. The direct light arrives in a straight line from light source without being scattered, while the diffuse light comes from several directions. The diffuse light arises from the scattering by small molecules (Rayleigh scattering) or larger particles (Mie scattering) in the atmosphere. Under the direct light, light distribution is bi-modally separated into bright and shaded parts, while the border between two parts is obscure under the diffuse light.

Previous studies suggested that plants use diffuse light more efficiently than direct light (Cohan et al., 2002; Gu et al., 2002; Farquhar and Roderick, 2003; Gu et al., 2003; Alton et al., 2007; Mercado et al., 2009; Li et al., 2014a, b) due to more homogenous light distribution inside canopy and non-linear saturation response of photosynthesis to light intensity. In greenhouses, shadings occurred by greenhouse structure, plant itself, and interactions between plants. Therefore, for improving light environment in greenhouses, diffuse covering materials such as diffuse film and glass which increase the diffuseness of light without affecting light transmission have been used (Hemming et al., 2007; 2008; 2014). Haze factor indicates the fraction of the direct light converted into diffuse light after passing covering materials (Li et al., 2014). Under the diffuse covering materials, plant growth and yield

increased (Hemming et al., 2007; Li et al., 2014a, b), and the effect on light distribution was evaluated (Li et al., 2014a). However, the effect of diffuse covering materials varied by location and season (Li and Yang, 2015).

Ray-tracing Simulation with 3D Plant Models

To examine spatial light distributions in a greenhouse and on plant canopy, ray-tracing simulation with a nested radiosity method (Chelle and Andrieu, 1998), Monte Carlo method (Veach, 1997; Cieslak et al., 2008), and reverse ray-tracing method (Bailey, 2018) have been applied. In the ray-tracing simulation, 3D plant models have been used to investigate the effect of plant structure, greenhouse equipment, seasonal variation, and plant arrangement (Buck-Sorlin et al., 2011; Sarlikioti et al., 2011a; de Visser et al., 2014; Kim et al., 2016; Jung et al., 2018).

Spatial light distribution of canopy strongly depends on plant architecture (Burgess et al., 2015), spatial leaf arrangement (Smith et al., 1989; Ross and Mottus, 2000), and leaf angle (Sarlikioti et al., 2011a). Therefore, the estimation accuracy of ray-tracing simulation differs by the accuracy of 3D plant models. However, most of 3D plant models had simple structures (Buck-Sorlin et al., 2011; Sarlikioti et al., 2011a; de Visser et al., 2014; Kim et al., 2016; Jung et al., 2018), which could not reflect the real structure of the plant. Recently, along with technical progress, high resolution 3D-scanning technologies have been developed. Through these technologies, accurate plant models could be reconstructed (Paulus et al., 2014; Zhang et al., 2016).

Canopy Photosynthesis Model

Canopy photosynthesis is crucial for crop growth and yield and thus various measurement methods have been developed using closed, semi-closed, and open chamber systems (Jarvis and Catsky, 1971; Field et al., 1989; Garcia, 1990; Shin et al., 2011; Kim et al., 2016). However, due to the complexity of measurement (Musgrave and Moss, 1961; Tranquillini, 1964; Billings et al., 1966; Denmead et al., 1993), mathematical models have been suggested to simply evaluate canopy photosynthesis under various conditions (Baldocchi DD and Amthor JS, 2001). Among them, the maximal productivity model, resource-use efficiency model, big-leaf model, sunlit-shaded model, and multi-layer model are well known (Zhu et al., 2012). These models vary in the amount of physiological and environmental mechanisms and details that they incorporate (Medlyn et al., 2003). The existing estimation models, although powerful tools, nevertheless have important constraints, which limit the accuracy in predicting canopy photosynthesis. For example, although, the basic concept that canopy photosynthesis models must separately account for diffuse and direct light has long been realized (Sinclair et al., 1976; Goudriaan, 1977), existing models predict the average light intensity on the assumption that light distribution in a canopy is homogeneous (Norman, 1980; de Pury and Farquhar, 1997), and estimate photosynthesis by simplifying complex plant metabolic processes. However, various forward and reverse ray-tracing algorithms

combined with 3D canopy architecture models have been developed to accurately predict the light environment inside the canopy (Chelle and Andrieu, 1998; Buck-Sorlin et al., 2011; Sarlikioti et al., 2011b; de Visser et al., 2014; Kim et al., 2016; Jung et al., 2018). And a number of kinetic models of photosynthesis and of plant primary metabolism have been developed and used for the estimation of canopy photosynthesis (Morgan and Rhodes, 2002; Laisk et al., 2006; Zhu et al., 2007; Ubierna et al., 2019).

MATERIALS & METHODS

3D-scanning and Reconstruction of 3D Plant Models

The tomato plants used for experiments were scanned to reconstruct 3D plant models (Fig. 1) with a high-resolution portable 3D scanner (GO! SCAN50[TM], CREAFORM, Lévis, Quebec, Canada). The resolution of the scanner was set at 2 mm. The 3D-scanned mesh obtained by 3D scanning was transformed into a parametric model using a scan software (Vxelement, CREAFORM) and a reverse engineering software (Geomagic Design X, 3D Systems, Rock Hill, SC, USA) and reconstructed in a 3D CAD software (SOLIDWORKS, Dassault systéms, Vélizy-Villacoublay, France).
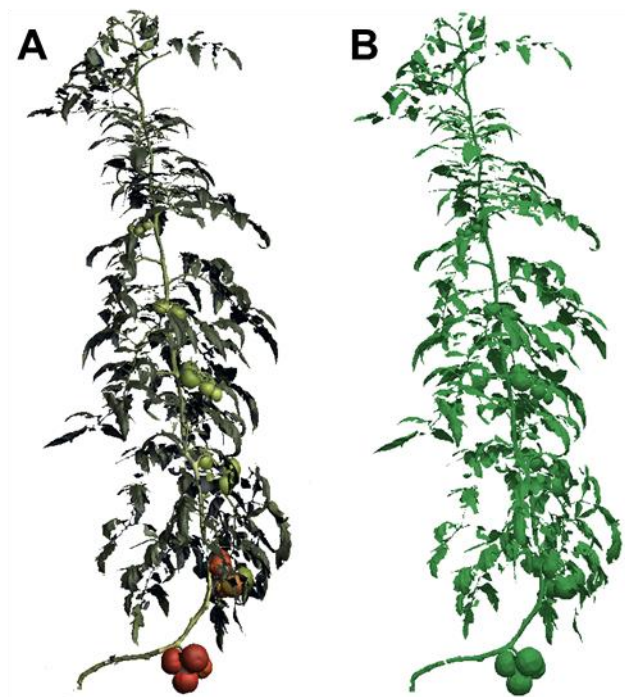
Fig. 1. 3D-scanned data (A) and reconstructed model (B) of the tomato plant.

Ray-tracing Simulation and Optical Modelling

Optisworks module (OPTISWORKS, OPTIS Inc., La Farléde, FRANCE) based on Monte-Carlo algorithm was used for optical-modelling and to simulate the solar distribution and trajectories of the sunlight rays inside the greenhouses and on the plants.

To apply optical properties of the 3D plant model in ray-tracing simulation, the light transmittance and reflectance were measured with a spectroradiometer (BLUE-Wave Spectrometer, StellarNet Inc., Tampa, FL, USA) combined with an integrating sphere (IC2, StellarNet Inc.). For plant, the measurement was conducted with nine randomly selected leaves from the top, middle, and bottom position of the plant canopy. Since leaf optical properties for different positions showed little differences, the average value of the nine leaves was used. The optical properties of the greenhouse structures were obtained with the same method. Optical properties from 400 to 700 nm were used in the ray-tracing simulation considering PAR (photosynthetically active radiation) (Appendix 1).

Accuracy Evaluation of the Ray-tracing Simulation

In order to evaluate the accuracy of the ray tracing simulation with 3D-scanned plant models, field measurements were conducted in greenhouses located at the Experimental Farm of Seoul National University in Suwon, Korea (37.3° N, 127.0° E). Light intensities were measured in the arch-type greenhouses (2 W × 3 L × 2 H, m). The greenhouses were covered with transparent (transmittance 95.26%, haze factor 17%) and opaque (transmittance 95.89%, haze factor 50%) diffuse films, respectively (Fig. 2A, B). Twelve tomato 'Dafnis' plants with average leaf area index (LAI) of 1.7 $m^2 \cdot m^{-2}$ were arranged in a planting density of two plants $\cdot m^{-2}$. Measurement was carried out during daytime on September 18, 2019 with quantum sensors (SQ-110, Apogee Instruments Inc., Logan, UT, USA) and a data logger (GL840, Graphtec Corp., Yokohama, Japan) in average interval of one hour. Measurements were conducted for one day to reconstruct 3D plant models without structural transformation versus to the plant structure at field measurement. Measurements were performed at heights of 0.5, 1.0 and 1.5 m with five horizontal positions at each height (Fig. 3).

Ray-tracing simulation was also conducted under a condition identical with the actual measurement condition. Tomato plants and greenhouse models were constructed in a 3D CAD software (SOLIDWORKS, Dassault systéms, Vélizy-Villacoublay, France). External direct and diffuse radiation was set the same with the values of the day (Appendix 2) measured with a sunshine sensor (BF5, Delta-T, Cambridge, UK).
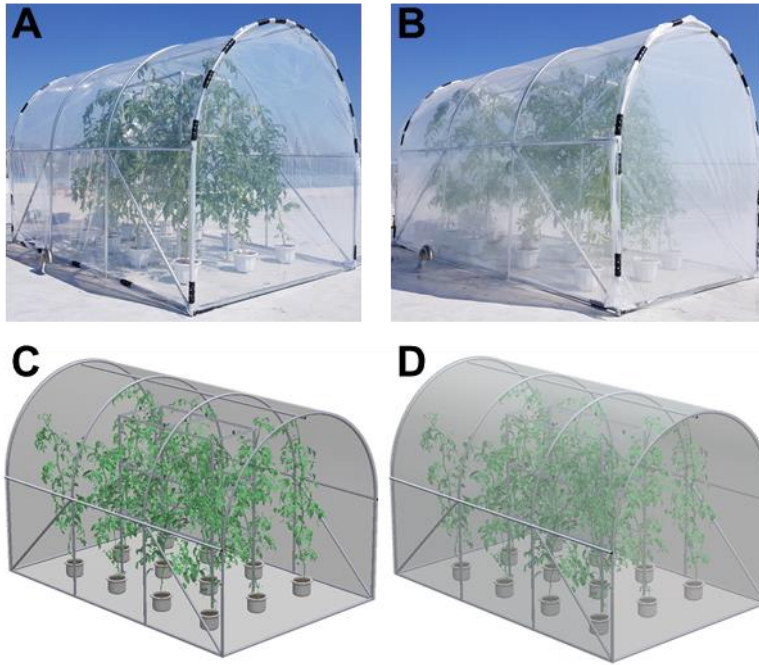
Fig. 2. Transparent (haze factor 17%, A) and opaque (haze factor 50%, B) greenhouses for actual measurement, and reconstructed models of transparent (C), and opaque (D) greenhouses for simulation.
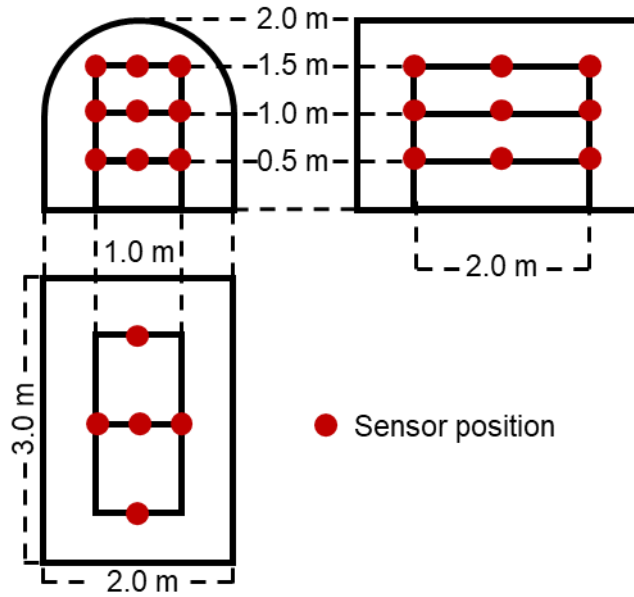
Fig. 3. Positions of quantum sensors for actual measurement inside the greenhouses. The sensors were located at three heights of 0.5, 1.0, and 1.5 m with five horizontal positions at each height.

Photosynthetic Rate and LUE Calculation

The whole canopy photosynthetic rate was calculated by absorbed PPFD obtained from optical simulation and canopy photosynthesis model. For photosynthesis model, modified Faquhar, von Caemmerer, and Berry (FvCB) model by Qian et al. (2012) was used. To obtain the FvCB model parameters, photosynthetic rate was measured at the top, middle, and bottom positions of the canopy by a portable photosynthesis system (LI-6400, LI-COR, Lincoln, NE, USA) with six different CO_2 concentrations (50, 100, 200, 400, 800, and 1200 $\mu mol \cdot mol^{-1}$) and eight different light intensities (0, 50, 100, 200, 400, 900, 1500, and 2000 $\mu mol \cdot m^{-2} \cdot s^{-1}$). Leaf temperature was set to 25°C and relative humidity ranged from 60 to 70% on the assumption that environmental conditions are fully controlled.

Photosynthetic rates were calculated by the FvCB model as follows:

$$P = \min(A_c, A_j) - R \qquad \text{(Eq. 1)}$$

$$A_c = \left(\frac{V_c(C_i - \Gamma^*)}{C_i + K_c\left(1 + \frac{O}{K_O}\right)} \right) \qquad \text{(Eq. 2)}$$

$$V_c = V_{cmax} \left(\frac{31 + \left(\frac{69}{1 + e^{-0.009(PAR - 500)}}\right)}{100} \right) \qquad \text{(Eq. 3)}$$

$$A_j = \left(\frac{J(C_i - \Gamma^*)}{4C_i + 8\Gamma^*} \right) \qquad \text{(Eq. 4)}$$

$$J = \left(\frac{\alpha PAR + J_{max} - \sqrt{(\alpha PAR + J_{max})^2 - 4\theta J_{max} \alpha PAR}}{2\theta} \right) \qquad \text{(Eq. 5)}$$

where P is leaf net assimilation rate (μmol $CO_2 \cdot m^{-2} \cdot s^{-1}$); R is non-photorespiratory respiration rate (μmol $CO_2 \cdot m^{-2} \cdot s^{-1}$), A_c and A_j are leaf gross assimilation rates limited by Rubisco activity (μmol $CO_2 \cdot m^{-2} \cdot s^{-1}$) and RuBP regeneration (μmol $CO_2 \cdot m^{-2} \cdot s^{-1}$), respectively; V_c is carboxylation capacity at specific light intensity (μmol $CO_2 \cdot m^{-2} \cdot s^{-1}$); PAR is photosynthetic photon flux density (PPFD, μmol $\cdot m^{-2} \cdot s^{-1}$); C_i is intercellular CO_2 concentration (μmol $\cdot mol^{-1}$); Γ^* is CO_2 compensation point (μmol $\cdot mol^{-1}$); K_C and K_O are Michaelis-Menten constants of Rubisco for CO_2 and O_2 (μmol $\cdot mol^{-1}$), respectively; O is oxygen concentration (μmol $\cdot mol^{-1}$); α is efficiency of light energy conversion on an incident light (μmol $\cdot mol^{-1}$); J_{max} is maximum electron transport rate (μmol $CO_2 \cdot m^{-2} \cdot s^{-1}$); and θ is curvature of light response of J (dimensionless) (Qian et al., 2012). Air temperature, relative humidity, and CO_2 concentration was assumed as 25℃, 60%, and 400 μmol $\cdot mol^{-1}$, respectively. V_{cmax} and J_{max} values of top, middle, and bottom leaf position in tomato plants were obtained as 83.5, 54.5, and 45.7, and 154.0, 104.4, and 86.4, respectively (Table 1).

LUE was calculated as a canopy photosynthetic rate divided by the amount of intercepted light.

Table 1. Maximum carboxylation capacity (V_{cmax}), maximum electron transport rate (J_{max}), non-photorespiratory respiration rate in Rubisco activity (R_{ac}) and RuBP regeneration limiting range (R_{aj}) of tomato plants in the FvCB model according to leaf position.

Parameter	Top	Middle	Bottom
V_{cmax}	83.5	54.5	45.7
J_{max}	154.0	104.4	86.4
R_{ac}	0.6	1.0	0.7
R_{aj}	0.4	0.5	0.6

Scenarios

For scenario analysis, arch-type virtual greenhouse models were constructed based on the standard design of Rural Development Administration, Korea (RDA, 2015) (Fig. 4). The 3D scanned plant models were arranged in rows with a planting density of two plants $\cdot m^{-2}$ in the greenhouse model. Tomato plants at 120 days after planting (DAT) were used because the shape of the canopy was almost constant during cultivation period after the stage due to the training and pruning system of the tomato plants. The LAI of the plants were 3.1 $m^2 \cdot m^{-2}$. For evaluating the effect of diffuse films, diffuse films with haze factors of 10%, 30%, 50%, 70%, and 90% with the same transmittance of 97.6% were optically-modelled (Fig. 5) and used to cover the virtual greenhouse models.

The effect of the diffuse film was evaluated in two main seasons of tomato harvest in Korea, summer and winter. External diffuse irradiance ratio of summer and winter were set as 50.1% and 25.7% respectively based on the data supplied by the Prediction Of Worldwide Energy Resources (NASA/POWER) project at NASA Langley Research Center (Fig. 6). Sun elevation angles of summer and winter seasons were set as 76.17° and 29.32° to represent the mid of the daytime. The inner-most three plants were used for analysis to represent common inter-canopy condition inside the greenhouse.
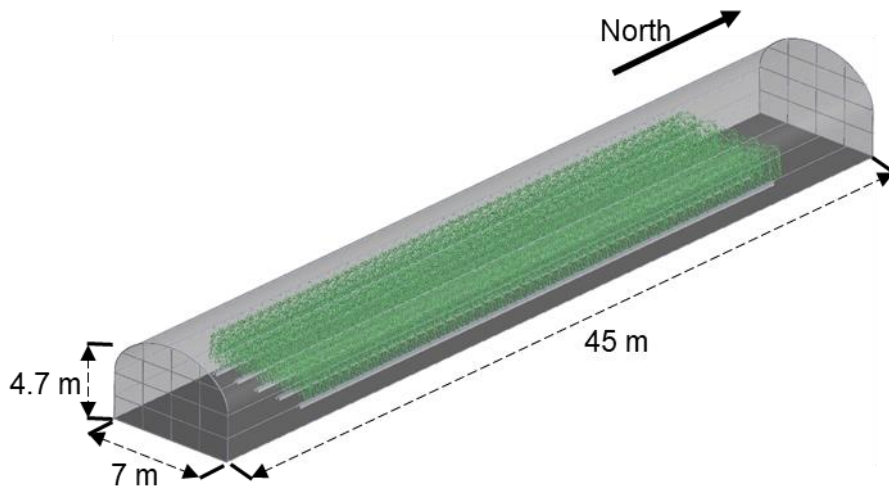
Fig. 4. A constructed arch-type greenhouse with the arrangement of 3D-scanned plant models.
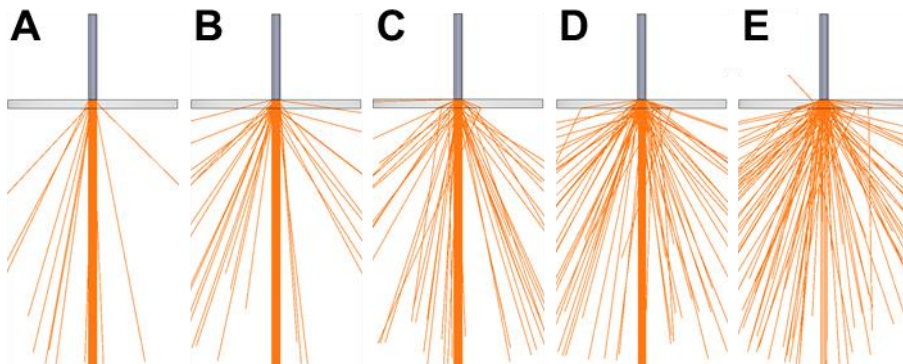
Fig. 5. Optically-modelled diffuse films with haze factors of 10% (A), 30% (B), 50% (C), 70% (D), and 90% (E). Light transmittances of all the films are the same.
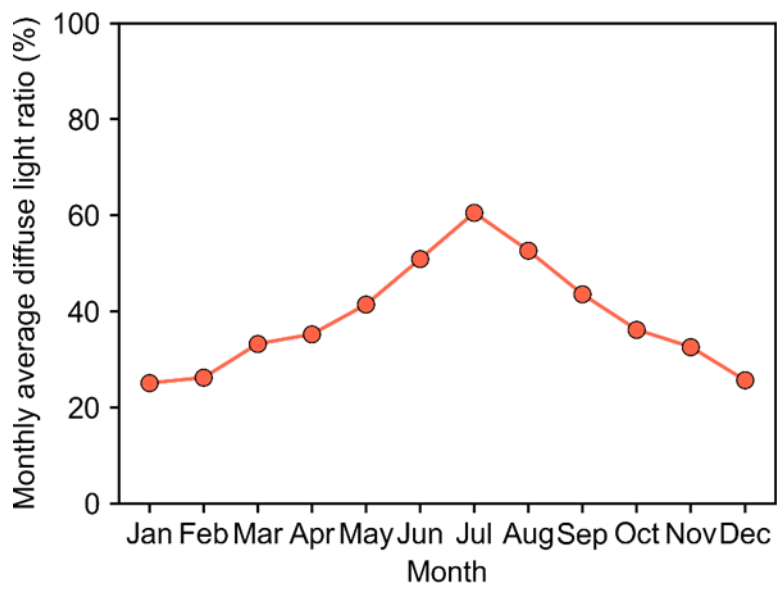
Fig. 6. Monthly change in average diffuse light ratio in Korea.

Statistical Analysis

Treatment effects on light distribution, photosynthesis, and LUE were evaluated by analysis of variance (ANOVA), using SPSS statistics, version 25.0 (IBM Corp. Armonk, NY, USA).

RESULTS

Accuracy Evaluation of Ray-tracing Simulation in Greenhouses

Fig. 7 shows a daily light intensity pattern measured at 15 points (three heights × five horizontal positions at each height) in greenhouses covered with haze factor 17% and 50% films, respectively. The measured and estimated light intensities showed good agreements with linear relationships (Fig. 8). However, the regression lines for greenhouses covered with haze factor 17% and 50% films were located above the 1:1 line, meaning that the simulated light intensity was slightly overestimated than measured one. The regression line located higher in greenhouse covered with haze factor 50% film than 17% film. The R^2 and mean absolute percentage error (MAPE) between the measurements and simulated results were 0.95 and 13.30%, and 0.94 and 17.85% in haze factor 17% and 50%, respectively.
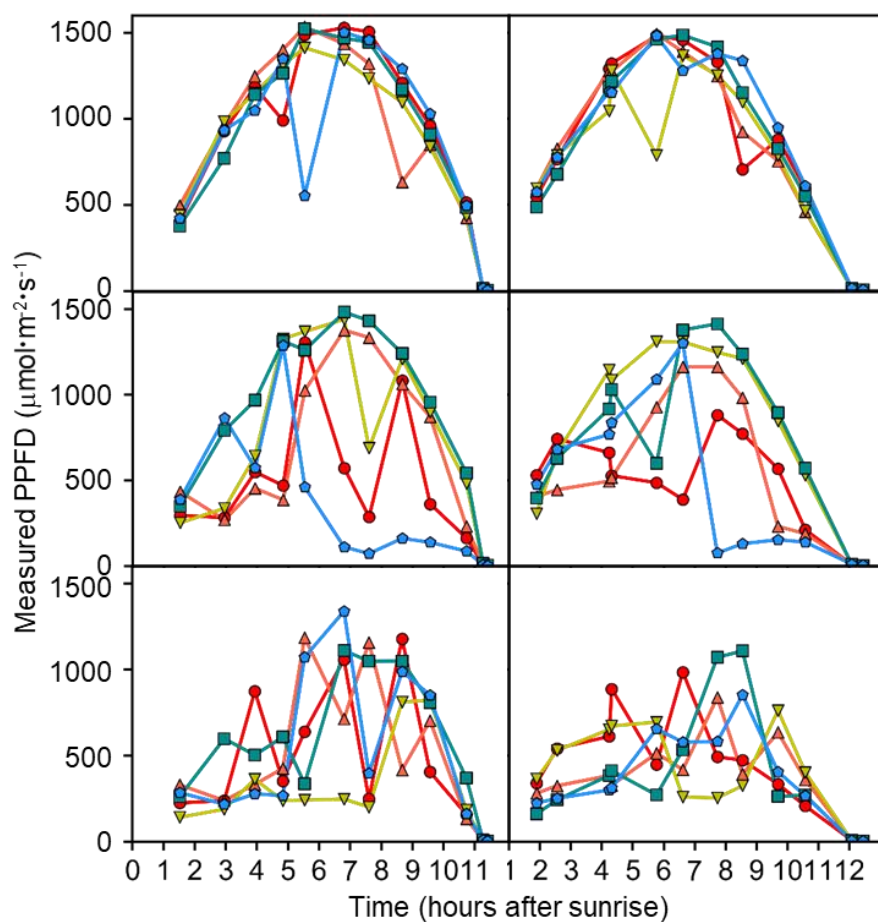
Fig. 7. Daily light intensity measured in greenhouses covered with haze factor 17% (left) and 50% (right) films. Light intensity measured at 1.5 m (upper), 1.0 m (middle), and 0.5m (lower) height. Each symbol represents the horizontal positions of sensors at each height. PPFD is photosynthetic photon flux density.

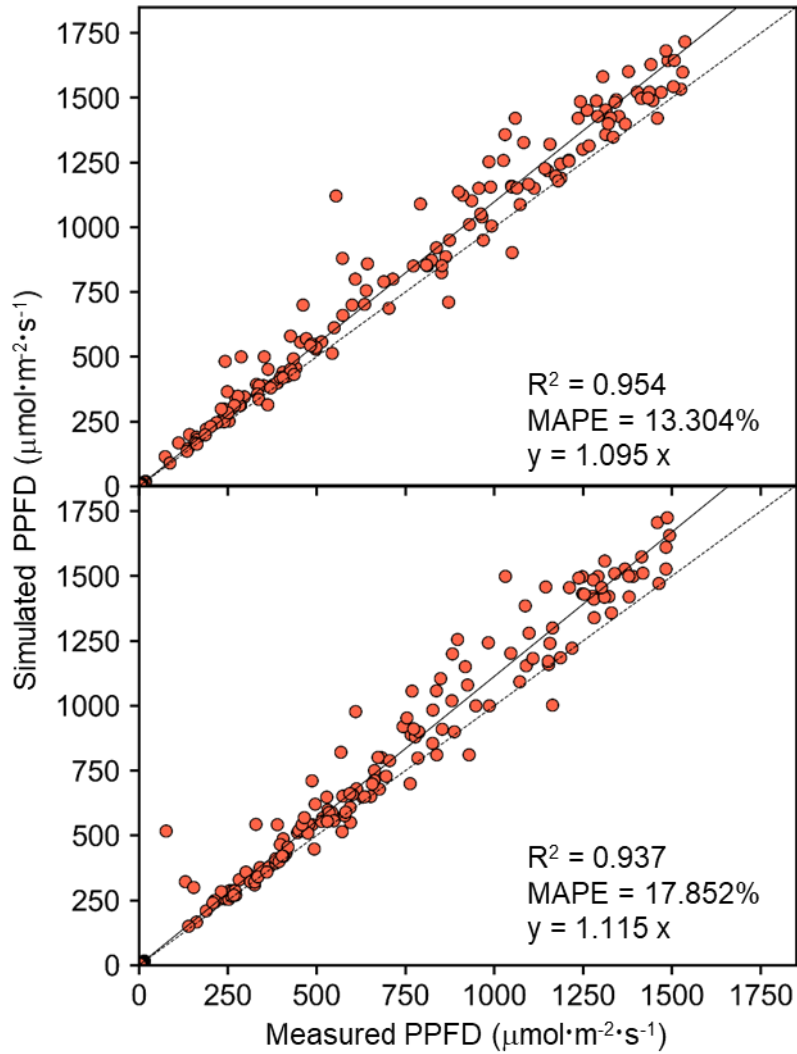Fig. 8. Comparison of measured and estimated light intensities in greenhouses covered with haze factor 17% (top) and 50% (bottom) diffuse films. Solid and dotted lines denote regression and 1:1 line, respectively. PPFD is photosynthetic photon flux density.

Light Distributions on Plants under Diffuse Films in Summer and Winter

The estimated results showed that the light was heterogeneously distributed on the surface of plant canopy, and the pattern was changed by seasonal condition and haze factor of diffuse film (Fig. 9). Absorbed amount of light by the plant was higher in summer than in winter. Even in the same season, spatial light distributions were changed by haze factor; however, showed no noticeable difference in summer. In winter, under the diffuse films with higher haze factors, the border between sunlit and shaded parts was ambiguous while the sunlight was distributed partially under the diffuse films with low haze factors.

Similar pattern was found in absorbed amount of light in summer and winter (Fig. 10). Both in summer and winter, the absorbed amount of light by the plant, top and middle layers maintained similar level under diffuse films with various haze factors (Fig. 10). However, the absorbed amount of light at the bottom layer decreased by 5.5% and 6.3% with increasing haze factor in summer and winter, respectively.

Different from absorbed amount of light, the standard deviation of absorbed light intensity showed different patterns in summer and winter (Fig. 10). In summer, standard deviation of absorbed light intensity of the plant, top, middle, and bottom layers showed no significant differences in all haze factors. However, in winter, the standard deviation decreased with increasing haze

26

factor, showing maximum decrease by 9.6%, 14.3%, 17.7%, and 18.4% in haze factor 90%.

Vertical and horizontal standard deviations of intercepted light intensities which indicate the heterogeneity of vertical and horizontal light distribution also showed different patterns in summer and winter (Fig. 11). In summer, the vertical and horizontal standard deviations increased in higher haze factor showing maximum increase by 4.6% and 1.0% respectively in haze factor 90%. However, in winter, vertical and horizontal standard deviations decreased with increasing haze factor showing maximum decrease by 5.7% and 10.0% respectively in haze factor 90%.

Extinction coefficient k, which represents a decreasing slope of light extinction from the top to the bottom of a canopy showed almost constant value along with haze factor changes in summer and winter (Fig. 12). The average of extinction coefficient k increased from 0.67 to 0.73 and 0.75 to 0.77 in summer and winter respectively, but there were no significant differences.
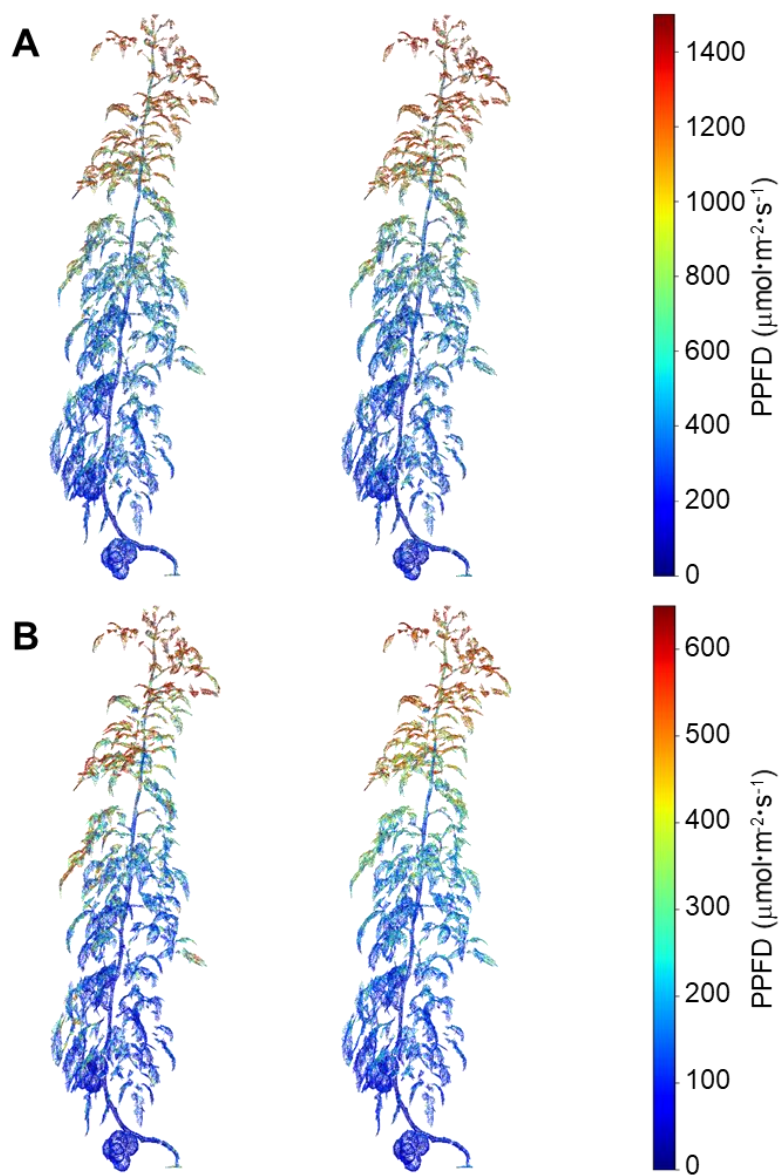
Fig. 9. Simulated spatial light distributions on 3D-scanned tomato models under
diffuse films: (A) in summer under diffuse film with haze factor 10% (left)
and 90% (right), (B) in winter under diffuse film with haze factor 10% (left)
and 90% (right). PPFD is photosynthetic photon flux density.
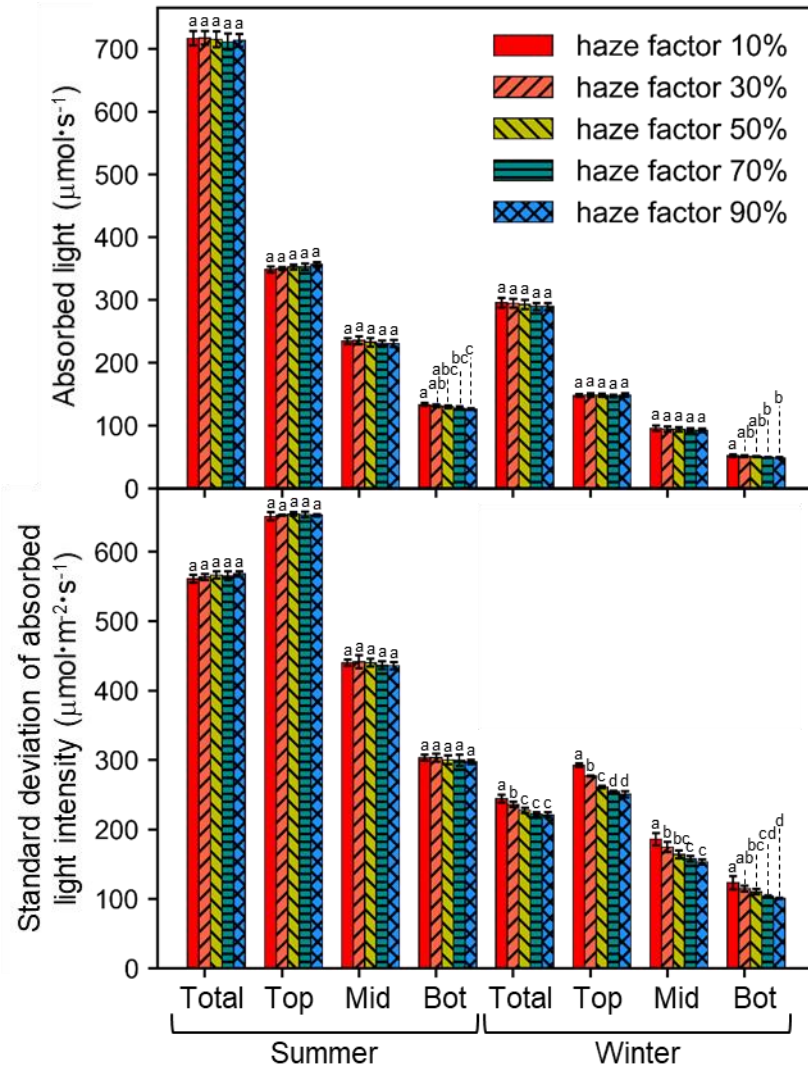
Fig. 10. Absorbed light and standard deviation absorbed light intensity of the total plant and top, middle, and bottom layers under diffuse films in summer and winter of Korea. Leaf areas of the top, middle, and bottom layers were 0.314, 0.466, and 0.469 m^2, respectively.
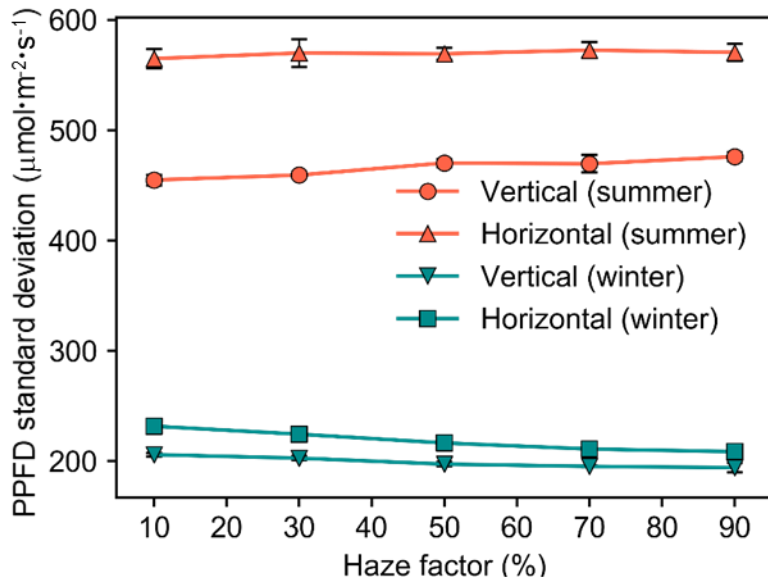
Fig. 11. The vertical and horizontal standard deviations of light interception by 3D-scanned tomato plant models under diffuse films according to haze factor (%) in summer and winter. PPFD is photosynthetic photon flux density.
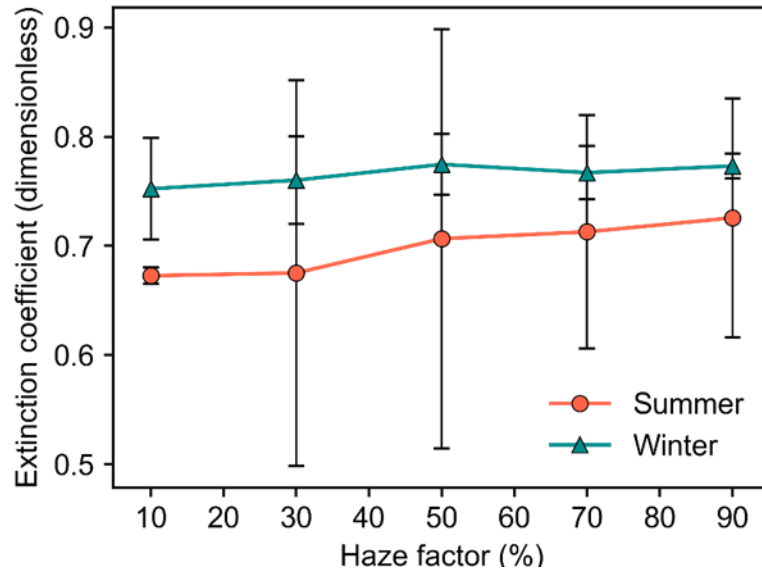
Fig. 12. Extinction coefficient k of 3D-scanned tomato plant models under diffuse films according to haze factor (%) in summer and winter.

Photosynthetic Rate and LUE of Plants Under Diffuse Films in Summer and Winter

The photosynthetic rate of a plant was generally higher in summer than in winter showing difference at the top, middle, and bottom layers (Fig. 13). The canopy photosynthetic rate was higher in summer, but LUE showed an opposite pattern.

In summer, photosynthetic rate of a plant did not increase along with haze factor increase; however, photosynthetic rate at the top and bottom layers increased and decreased by 1.3% and 5.7%, respectively. Different from photosynthetic rate, LUE was not affected by haze factor in summer. In winter, with increasing haze factor, photosynthetic rate of a plant increased 1.9%, but there was no significant difference, while photosynthetic rate at the top layer increased by 3.9% significantly. Contrary to LUE in summer, LUE noticeably increased in winter along with haze factor increase. With increasing haze factor, LUE of the plant, top, middle, and bottom layers increased 3.9%, 3.1%, 3.6%, and 5.2%, respectively.
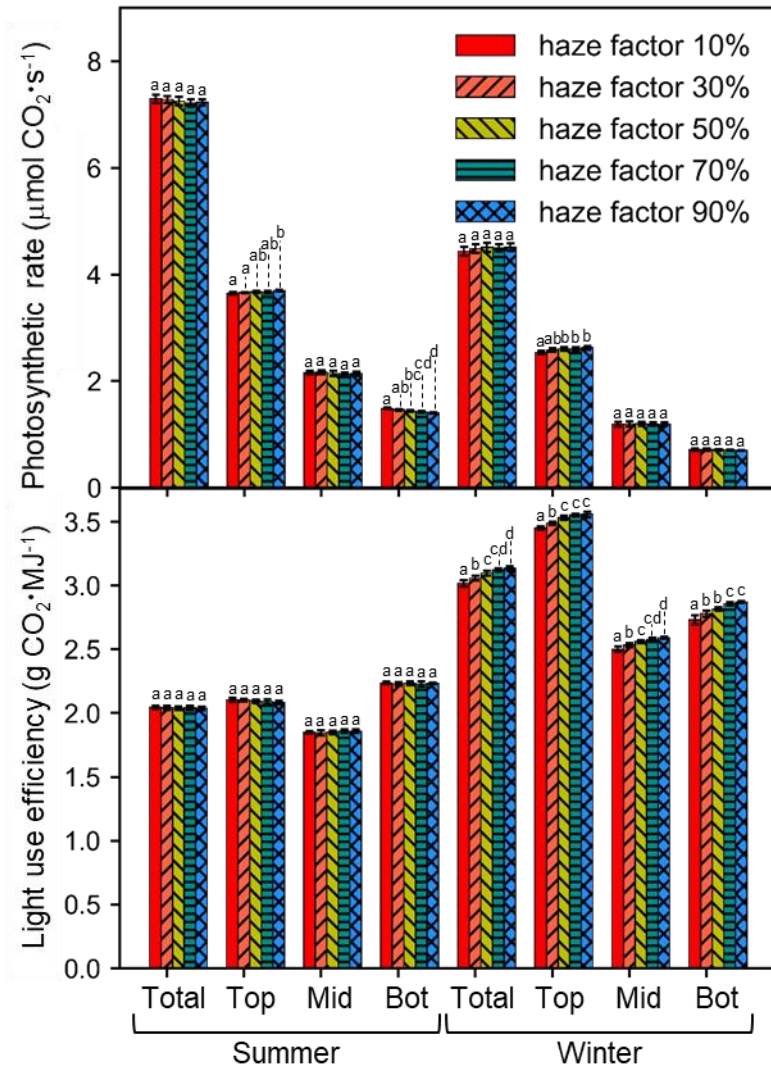
Fig. 13. Photosynthetic rate and light use efficiency of the total plant and top, middle, and bottom layers under diffuse films in summer and winter of Korea. Leaf areas of the top, middle, and bottom layers were 0.314, 0.466, and 0.469 m^2, respectively.

DISCUSSION

Accuracy of Ray-tracing Simulation in Greenhouses

The ray-tracing module used in this study (OPTISWORKS, OPTIS Inc., La Farléde, FRANCE) employs Monte-Carlo algorithm which is well-known methodology for robust simulation. The ray-tracing module has been utilized for solar energy analysis and light interception estimation (Ali et al., 2010; Hasna, 2011; Arnaoustakis et al., 2015; Daabo et al., 2016, 2019). The Optisworks ray-tracing module was validated (Sellami N, 2013; Daabo et al., 2016, 2017) and recognized as one of the reliable tools for solar design and ray-tracing simulation (Jakica N, 2018).

In this study, the simulated light intensities showed good agreements with the measured ones (Fig. 8), indicating that the ray-tracing simulation with 3D-scanned plant models is capable of well estimating light distribution under diffuse films in greenhouses and on plants. However, the simulated light intensity was slightly overestimated than measured one. The overestimation could be attributed to the difference between real sensor and virtual sensor implemented in simulation. Most of the quantum sensors usually have some errors and tend to under-measure when the incoming angle of incident light is closer to the parallel line of the detecting surface of the sensor. Thus, there have been very few studies that used virtual sensors to measure irradiance (Buck-sorlin et al., 2011; Tian et al., 2017) with specific adaptations for the sensor

(Hitz et al., 2019). In many studies, estimated light intensity usually showed tendency to be higher than actual light intensity (Hitz et al., 2019; Pakari and Ghani 2019). The higher regression line in the greenhouse covered with diffuse film with haze factor 50% than 17% also could be attributed to the same reason.

Changes in Light Distribution by Haze Factor and Seasonal Condition

The light distribution on plants was changed by haze factor of diffuse film both in summer and winter (Fig. 9, 10). Light distribution on plants tends to be homogeneous under diffuse light (Farquhar and Roderick, 2003). Similarly, in winter, the light profile was homogeneous at higher haze factor showing lower standard deviation of absorbed light intensity, while the homogeneity did not increase in summer (Fig. 10). The difference between summer and winter could be attributed to the external diffuse irradiance ratio which were set differently to 50.1% and 25.7% for summer and winter, respectively. Diffuse irradiance ratio inside a greenhouse which is determined by external diffuse irradiance and haze factor of diffuse film can be easily saturated in a condition with higher external diffuse irradiance ratio. For this reason, the effect of diffuse films on light distribution could be diminished in summer than in winter.

Both in summer and winter, vertical standard deviation was less affected by haze factor (Fig. 11), which is in consistent with Acock et al. (1970) who concluded that the heterogeneity of light distribution on the horizontal plane highly increases with decreasing diffuse fraction of sunlight. Also, similar result was reported by Li et al. (2014a) that the horizontal and vertical light distributions accounted for large and relatively small amount of the effect of diffuse covering materials on tomato plants, respectively.

Diffuse light usually exhibits a lower extinction coefficient k than direct light, which represents a deeper light penetration into a canopy (Urban et al., 2007; Li et al., 2014a). However, the increase in haze factor of diffuse film resulted no significant difference both in summer and winter (Fig. 12). The result can be explained by sun elevation angle and external diffuse irradiance ratio. Several researches suggested that the lower extinction coefficient k is usual, but not absolute phenomenon which can be differed by solar elevation angle (Morris 1989, Sarlikioti et al., 2011b) and external meteorological condition (Li et al., 2014).

Through the method suggested in this study, light distributions under diffuse films could be estimated, which was consistent with previous studies. Thus, this method was confirmed to be reliable for analyzing the effect of diffuse films on light interception of tomato plants. Besides, the light distributions could be analyzed not only at canopy-scale but also at small scales in various environmental conditions with time and labor savings.

Changes in Photosynthetic Rate and LUE by Haze Factor and Seasonal Condition

The photosynthetic rate of tomato plants was not changed significantly by haze factor both in summer and winter (Fig. 13). However, the average of photosynthetic rate of a plant increased by 1.9% with increasing haze factor while no particular trend was found in summer. The effect of higher haze factor on photosynthetic rate in summer could be attributed to the higher external diffuse irradiance ratio resulted by the long rainy season in summer of Korea. In contrast, the beneficial effect of higher haze factor in winter could be attributed to the lower external diffuse irradiance ratio resulted by clear weather in winter of Korea. Based on the estimated photosynthesis, the application of diffuse film with high haze factor seems to be ineffective and beneficial in summer and winter, respectively. In previous research, photosynthetic rate increased under diffuse light condition in a sparse and dense woodland about 12% and 22% respectively (Alton et al., 2007). Also, Li et al. (2014a) concluded that canopy photosynthetic rate of a densely cultivated tomato plants increased 7.2% under diffuse film versus to clear film on clear day (Li et al., 2014a). Considering that a low LAI decreases the potential effect of diffuse light (Li and Yang., 2015) and the greenhouse tomato plants of this scenario have a lower LAI, the increases in photosynthetic rate in this result seem to be reasonable. However, since photosynthetic rate of tomato plants highly

influenced by temperature (Bar-Tsur et al., 1985; Camejo et al., 2005), the robustness of the photosynthetic rate estimation could be improved by considering local temperature distribution inside greenhouse.

Under diffuse light, LUE tends to become higher due to non-linear light saturation response of photosynthesis (Marshall and Biscoe, 1980). Similarly, LUE increased notably with increasing haze factor in winter with lower standard deviation of absorbed light intensity, which can contribute to the evasion of light saturation in photosynthesis (Fig. 10, 11). On the contrary, LUE did not increased in summer due to the almost constant standard deviation caused by high external diffuse irradiance ratio.

The method suggested in this study could estimate canopy photosynthesis and LUE under diffuse films, which seem reasonable compared to previous studies. Therefore, we believe that this method can analyze the effect of diffuse films on canopy photosynthesis and LUE of tomato plants without time and space constraints, and evaluate the applicability of diffuse films to various regions and seasons.

CONCLUSION

In this study, a novel method estimating light interception and photosynthesis of tomato plants under various diffuse films was proposed by using 3D-scanned plant model, photosynthesis model, and ray-tracing simulation. The reliability of this method was evaluated by comparing actual measured and simulated light intensities in the greenhouse, which showed good agreements. Various light distribution patterns including standard deviations and extinction coefficient k showed the results similar to previous studies. Furthermore, applicability of diffuse films was evaluated and the calculated canopy photosynthetic rate and LUE changed in reasonable ranges with increasing diffuse light. Through this method, canopy light distribution, photosynthetic rate, and LUE can be estimated with time and labor savings and without time and space limitations. This method can be used not only to quantify canopy light interception and photosynthetic rate under various diffuse films, but also to select optimum diffuse films for various regions.

LITERATURE CITED

Acock B, Thomley JHM, Warren Wilson J (1970) Spatial variation of light in the canopy. In: Setliik I (ed) Prediction and measurement of photosynthetic productivity, Proceedings of the IBP/PP technical meeting, Trebon, 14-21 September 1969, PUDOC, Wageningen, 91-102

Ali IMS, Mallick TK, Kew PA, O'Donovan TS, Reddy KS (2010) Optical performance evaluation of a 2-D and 3-D novel hyperboloid solar concentrator, In: Sayigh A (ed) Proceedings of the 11th World Renewable Energy Congress, Abu Dhabi, UAE, 2010

Alton PB, North PR, Los SO (2007) The impact of diffuse sunlight on canopy light use efficiency, gross photosynthetic product and net ecosystem exchange in three forest biomes. Glob Chang Biol 13:776-787

Arnaoutakis GE, Marques-Hueso J, Ivaturi A, Fischer S, Goldschmit JC, et al. (2015) Enhancement energy conversion of up-conversion solar cells by the integration of compound parabolic concentrating optics. Sol Energy Mater Sol Cells 140:217-223

Bailey BM (2018) A reverse ray-tracing method for modelling the net radiative flux in leaf-resolving plant canopy simulations. Ecol Model 368:233-245

Baldocchi DD, Amthor JS (2001). Terrestrial global productivity. In: Baldocchi DD, Amthor JS (eds) Canopy photosynthesis: history, Academic Press, New York, pp 9-31

Bar-Tsur A, Rudich J, Bravdo B (1985) Photosynthesis, transpiration and stomatal resistance to gas exchange in tomato plants under high temperature. J Hortic Sci 60:405-410

Billings WD, Clebsch EEC, Mooney HA (1966) Photosynthesis and respiration rates of Rocky Mountain alpine plants under field conditions. Am Midland Natural 75:34-44

Borger CPD, Hashem A, Pathan S (2010) Manipulating crop row orientation to suppress weeds and increase crop yield. Weed Sci 58:174-178

Buck-Sorlin G, de Visser PHB, Henke M, Sarlikioti V, van der Heijden GW, Marcelis LFM, Vos J (2011) Towards a functional–structural plant model of cut-rose: simulation of light environment, light absorption, photosynthesis and interference with the plant structure. Ann Bot 108:1121-1134

Burgess AJ, Retkute R, Herman T, Murchie EH (2017) Exploring relationships between canopy architecture, light distribution, and photosynthesis in contrasting rice genotypes using 3D canopy reconstruction. Front Plant Sci 8:734

Burgess AJ, Retkute R, Pound MP, Foulkes J, Preston SP, Jensen OE, Pridmore TP, Murchie EH (2015) High-resolution three-dimensional structural data quantify the impact of photoinhibition on long-term carbon gain in wheat canopies in the field. Plant Physiol 169:1192-1204

Camejo D, Rodriguez P, Morales MA, Dell'Amico JM, Torrecillas A et al. (2005) High temperature effects on photosynthetic activity of two tomato cultivars with different heat susceptibility. J Plant Physiol 162(3):281-289

Chelle M, Andrieu B (1998) The nested radiosity model for the distribution of light within plant canopies. Ecol Model 111:75-91

Choudbury B (2001) Estimating gross photosynthesis using satellite and ancillary data: approach and preliminary results. Remote Sens Environ 75:1-21

Cieslak M, Lemieux C, Hanan J, Prusinkiewicz P (2008) Quasi-Monte Carlo simulation of the light environment of plants. Funct Plant Biol 35:837-849

Cohan DS, Xu J, Greenwald R, Bergin MH, Cahmeides WL (2002) Impact of atmospheric aerosol light scattering and absorption on terrestrial net primary productivity. Global Biogiochem Cycles 16: 37-1

Daabo AM, AI-Mola YS, AI-Rawy AY, Lattimore T (2019) State of the art single-objective optimization of small scale cylindrical cavity receiver. Sustain Energy Technol Assess 35:278-290

Daabo AM, Mahmoud S, AI-Dadah RK (2016) The effect of receiver geometry on the optical performance of a small-scale solar cavity receiver for parabolic dish applications. Energy 144:513-525

Daabo AM, Mahmoud S, AI-Dadah RK, Ahmad A (2017) Numerical investigation of pitch value on thermal performance of solar receiver for solar powered Brayton cycle application. Energy 119:523-539

Denmead OT, Dunin FX, Wong SC, Greenwood EAN (1993) Measuring water use efficiency of Eucalypt trees with chambers and micrometeorological techniques. J Hydrol 150:649-664

dePury DGG, Farquhar GD (1997) Simple scaling of photosynthesis from leaves to canopies without the errors of big-leaf models. Plant Cell Environ 20:537-557

de Visser, PHB, van der Heijden, GW, Buck-Sorlin, G (2014) Optimizing illumination in the greenhouse using a 3D model of tomato and a ray tracer. Front Plant Sci 5:48

Farquhar GD, Roderick ML (2003) Pinatubo, diffuse light, and the carbon cycle. Science 299(5615):1997-1998

Field CB, Ball JT, Berry JE (1989) Photosynthesis: Principles and field techniques. In: Pearcy RW, Ehleringer JR, Mooney HA, Rundel PW (eds) Plant physiological ecology: Field methods and instrumentation, Springer, Dordrecht, pp 209-253

Garcia RL, Norman JM, Medermitt DK (1990) Measurements of canopy gas exchange using an open chamber system. Remote Sensing Reviews 5:141-162

Gonzalez-Real MM, Baille A, Gutierrez Colomer RP (2007) Leaf photosynthesis properties and radiation profiles in a rose canopy (*Rosa hybrid* L.) with bent shoots. Sci Hortic 114:177-187

Goudriaan J (1977) Crop micrometeorology: a simulation study. Dissertation, Wageningen UR

Gu L, Baldocchi DD, Verma SB, Black TA, Vesala T, Falge EM (2002) Advantages of diffuse radiation for terrestrial ecosystem productivity. J Geophys Res 107 (D6):ACL2-1 to 2-23

Gu L, Baldocchi DD, Wofsy SC, Munger JW, Michalsky JJ, Urbanski SP (2003) Response of deciduous forest to the Mount Pinatubo eruption: enhanced photosynthesis. Science 299:2035-2038

Hasna G (2011) Solar energy concentrators and their optimization and analysis with the optisworks solar package. In: Omatsu T (ed) Proceedings of renewable energy and the environment, Texas, USA, 2011

Hemming S, Duek TA, Janse J, van Noort F (2007) The effect of diffuse light on crops. Acta Hortic 801:1293-1300

Hemming S, Mohammadkhani V, Dueck TA (2008) Diffuse greenhouse covering materials-material technology, measurements and evaluation of optical properties. Acta Hortic 797:469-475

Hemming S, Mohammadkhani V, van Ruijven J (2014) Material technology of diffuse greenhouse covering materials – influence on light transmission, light scattering and light spectrum. Acta Hortic 1037:883-895

Henke M, Buck-Sorlin, GH (2018) Using a full spectral raytracer for calculating light microclimate in functional-structural plant modelling. Comput Inform 36:1492-1522

Hitz T, Henke M, Graeff-Honninger S, Munz S (2019) Three-dimensional simulation of light spectrum and intensity within an LED growth chamber. Comput Electron Agric 156:540-548

Hoagland DR, Arnon DI (1950) The water culture method for growing plants without soil. Calif Agric Exp Stn Bull. 347:36-39

Hollinger DY, Kelliher FM, Byers JN, Hunt JE, McSevery TM, Wier PL (1994) Carbon dioxide exchange between an undisturbed old-growth temperate forest and the atmosphere. Ecology 75:134-150

Jakica N (2018) State-of-the-art review of solar design tools and methods for assessing daylighting and solar potential for building-integrated photovoltaics. Renew Sustain Energy Rev 81:1296-1328

Jarvis PG, Catsky J (1971) General principles of gasometric methods and the main aspects of installation design. In: Sestak Z, Catsky J, Jarvis PG (eds) Plant Photosynthetic Production: Manaual of Methods. Dr. W. Junk NV, The Hague, pp.49-110

Jung D, Lee J, Kang W, Hwang I., Son J (2018) Estimation of whole plant photosynthetic rate of irwin mango under artificial and natural lights using a three-dimensional plant model and ray-tracing. Int J Mol Sci 19:152

Kim JH, Lee JW, Ahn TI, Shin JH, Park KS, Son JE (2016) Sweet pepper (*Capsicum annuum* L.) canopy photosynthesis modeling using 3D plant architecture and light ray-tracing. Front Plant Sci 7:1321

Knohl A, Baldocchi DD (2008) Effects of diffuse radiation on canopy gas exchange processes in a forest ecosystem. J Geiophys Res Biogeosci, 113: G2

Laisk A, Eichelmann H, Oja V (2006) C3 photosynthesis in silico. Photosynth Res 90:45-66

Li T, Heuvelink E, Dueck TA, Janse J, Gort G, Marcelis LFM (2014a) Enhancement of crop photosynthesis by diffuse light: quantifying the contributing factors. Ann Bot 114:145-156

Li T, Heuvelink E, van Noort F, Kromdijk J, Marcelis LFM (2014b) Responses of two *Anthurium* cultivars to high daily integrals of diffuse light. Sci Hortic 179:306-313

Li T, Yang Q (2015) Advantages of diffuse light for horticultural production and perspectives for further research. Front Plant Sci 6:704

Marshall B, Biscoe PV (1980) A model for C3 leaves describing the dependence of net photosynthesis on irradiance. J Exp Bot 31:29-39

Mdelyn B, Barrett D, Landsberg J, Sands P, Clement R (2003) Conversion of canopy intercepted radiation to photosynthate: review of modelling approaches for regional scales. Funct Plant Biol 30:153-169

Medlyn B, Barrett D, Landsberg J, Sands P, Clement R (2003) Corrigendum to: Conversion of canopy intercepted radiation to photosynthate: a review of modelling approaches for regional scales. Funct Plant Biol 30:829-829

Mercado LM, Bellouin N, Sitch S, Boucher O, Huntingford C, Wild M (2009) Impact of changes in diffuse radiation on the global land carbon sink. Nature 458:1014-1017

Morgan JA and Rhodes D (2002) Mathematical modeling of plant metabolic pathways. Metab Eng 4:80-89

Musgrave RB, Moss DN (1961) Photosynthesis under field condition．Ⅰ．A portable, closed system for determining the rate of photosynthesis and respiration in corn. Crop Sci 1:37-41

Niinemets U (2007) Photosynthesis and resource distribution through plant canopies. Plant Cell Environ 30:1052-1071

Norman JM (1980) Interfacing leaf and canopy light interception models. Predicting photosynthesis for ecosystem models. In: Hesketh JD, Jones JW (eds) Plant photosynthesis, CRC Press, Florida, pp 49-67

Pakari A, Ghani S (2019) Evaluation of a novel greenhouse design for reduced cooling loads during the hot season in subtropical regions. Sol Energy 181:234-242

Paulus S, Schumann H, Kuhlmann H, Leon J (2014) High-precision laser scanning system for capturing 3D plant architecture and analyzing growth of cereal plants. Biosyst Eng 121:1-11

Qian T, Elings A, Dieleman JA, Gort G, Marcelis LFM (2012) Estimation of photosynthesis parameters for a modified Farquhar–von Caemmerer–

Berry model using simultaneous estimation method and nonlinear mixed effects model. Environ Exp Bot 82:66-73

Roderick ML, Farquhar GD, Berry SL, Noble IR (2001) On the direct effect of clouds and atmospheric particles on the productivity and structure of vegetation. Oecologia 129:21-30

Ross J, Mottus M (2000) Statistical treatment of sunfleck length inside the willow coppice. Agric For Meteorol 104:215-231

Rural Development Administration (2015) Disaster-proof standard designs and specifications for horticulture facilities: plastic greenhouse, ginseng and mushroom cultivation facility, Jinhan M&B, Seoul

Sarlikioti V, de Visser PH, Marcelis LFM (2011a) Exploring the spatial distribution of light interception and photosynthesis of canopies by means of a functional–structural plant model. Ann Bot 107:875-883

Sarlikioti V, de Visser PH, Buck-Sorlin GH, Marcelis LFM (2011b) How plant architecture affects light absorption and photosynthesis in tomato: towards an ideotype for plant architecture using a functional-structural plant model. Ann Bot 108:1065-1073

Sellami N (2013) Design and characterization of a novel translucent solar concentrator. Dissertation, Heriot-Watt university

Shin JH, Ahn TI, Son JE (2011) Quantitative measurement of carbon dioxide consumption of a whole Paprika plant (*Capsicum annuum* L.) using a large sealed chamber. Kor J Hort Sci Tech 29.3:211-216

Sievanen R, Godin C, DeJong TM, Nikinmaa E (2014) Functional–structural plant models: a growing paradigm for plant studies. Ann Bot 114:599-603

Sinclair TR, Murphy CE, Knoerr KR (1976) Development and evaluation of simplified models for simulating canopy photosynthesis and transpiration. J Appl Ecol 13:813-829

Smith WK, Knapp AK, Reiners WA (1989) Penumbral effects on sunlight penetration in plant communities. Ecology 70:1603-1609

Tian T, Wu L, Henke M, Ali B, Zhou W, Buck-Sorlin G (2017) Modelling allometric relationships in leaves of young rapeseed (*Brassica napus* L.) grown at different temperature treatment. Front Plant Sci 8:313

Townsend AJ, Retkute R, Chinnathambi K, Randall JW, Foulkes J, Carmo-Silva E, Murchie EH (2018) Suboptimal acclimation of photosynthesis to light in wheat canopies. Plant Physiol 176:1233-1246

Tranquillini W (1964) Photosynthetic and dry matter production of trees at high altitudes. In: Zimmermann MH (ed) The formation of wood in forest trees, Academic Press, Cambridge, pp 505-518

Ubierna N, Cernusak LA, Holloway-Phillips M, Busch FA, Cousins AB, Farquhar GD (2019) Critical review: incorporating the arrangement of mitochondria and chloroplast into models of photosynthesis and carbon isotope discrimination. Photosynth Res 1-27

Urban O, Janous D, Acosta M, Czerny R, Markova I, NavrATil M, et al. (2007) Ecophysiological controls over the net ecosystem exchange of mountain

spruce stand. Comparison of the response in direct vs. diffuse solar radiation. Glob Chang Biol 13:157-168

Urban O, Klem K, Ac A, Havrankova K, Holissova P, Navratil M, et al., (2012) Impact of clear and cloudy sky conditions on the vertical distribution of photosynthetic CO2 uptake within a spruce canopy. Funct Ecol 16:46-55

Veach E (1997) Robust Monte Carlo methods for light transport simulation. Dissertation, Stanford University

Zhang M, Yu GR, Zhuang J, Gentry R, Fu YL, Sun XM, et al. (2011) Effects of cloudiness change on net ecosystem exchange, light use efficiency, and water use efficiency in typical ecosystems of China. Agric For Meteorol 151:803-816

Zhang Y, Teng P, Shimizu Y, Hosoi F, Omasa K (2016) Estimating 3D leaf and stem shape of nursery paprika plants by a novel multi-camera photography system. Sensors 16:874

Zhu XG, de Sturler E, Long SP (2007) Optimizing the distribution of resources between enzymes of carbon metabolism can dramatically increase photosynthetic rate: a numerical simulation using an evolutionary algorithm. Plant Physiol, 145:513-526

Zhu XG, Song Q, Ort DR (2012) Elements of a dynamic systems model of canopy photosynthesis. Curr Opin Plant Biol 15.3:237-244

ABSTRACT IN KOREAN

최근 온실 내 광분포 개선을 통한 광이용효율 증대를 위해 산란피복재가 사용되고 있다. 산란피복재의 효과는 수식 모델과 실측 방식에 의하여 평가되고 있으나 작물을 기준으로 광 분포를 정확하게 측정할 수 없고 제한된 환경 조건에서만 적용할 수 있는 단점이 있다. 본 연구의 목적은 토마토 수광분포 및 광합성속도에 대한 산란필름의 효과를 다양한 환경 조건 하에서 3 차원 스캔 식물모델과 광추적 시뮬레이션을 이용하여 정량적으로 평가하는 것이다. 광 추적 시뮬레이션의 신뢰성을 확인하기 위해 작물이 있는 투명 및 확산필름 피복 온실 내부에 총 15 개 (5 개 x 3 단)의 광센서를 설치하여 측정한 광도와 시뮬레이션을 통한 추정된 광도를 비교하였다. 또한, 한국의 주요 토마토 수확 계절인 여름과 겨울에서의 온실 내 광분포를 각 계절별 태양입사각과 산란비를 반영하여 추정하였고, 이를 기반으로 광합성속도를 계산하였다. 실제와 동일하게 구현된 환경에서 추정된 온실 내 광도는 투명 및 산란필름 피복 온실에서 각각 R^2=0.954, 0.937 을 보이며 측정값과 잘 일치하였다. 외부 산란비가 높은 여름에는 광합성속도와 광이용효율의 추정값이 haze factor 증가에 따른 변화 경향성을 보이지 않았다. 반면, 외부 산란비가 낮은 겨울에는 haze factor 가

증가함에 따라 광합성속도와 광이용효율 각각 최대 1.8%, 3.9%
증가하였으나, 유의한 차이는 없었다. 본 연구 결과는 다양한
산란필름 하에서의 작물 수광분포 및 광합성속도를 정량화 하는데
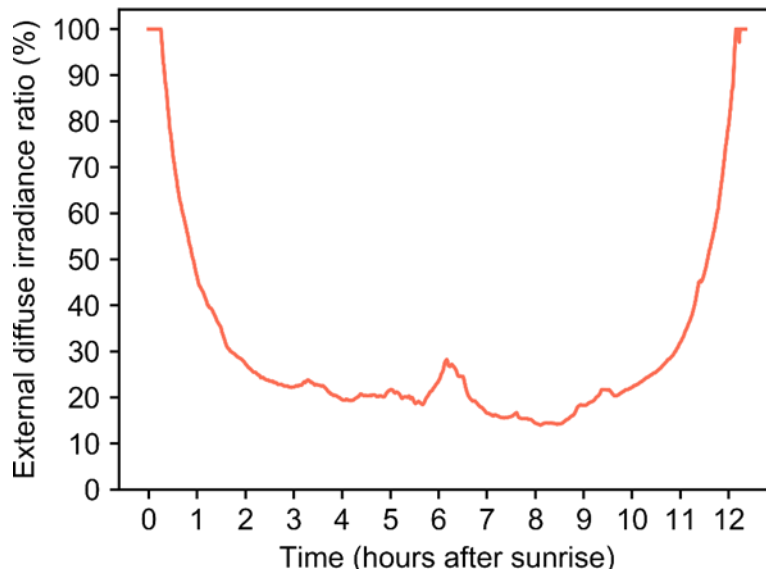사용될 뿐 아니라, 지역별 최적의 산란필름을 선정하는데 사용될 수
있을 것이다.

추가 주요어: 몬테카를로 방법, 확산광, 태양광, 3 차원 스캔, 산란광
비율

학　번: 2018−26599

APPENDICES
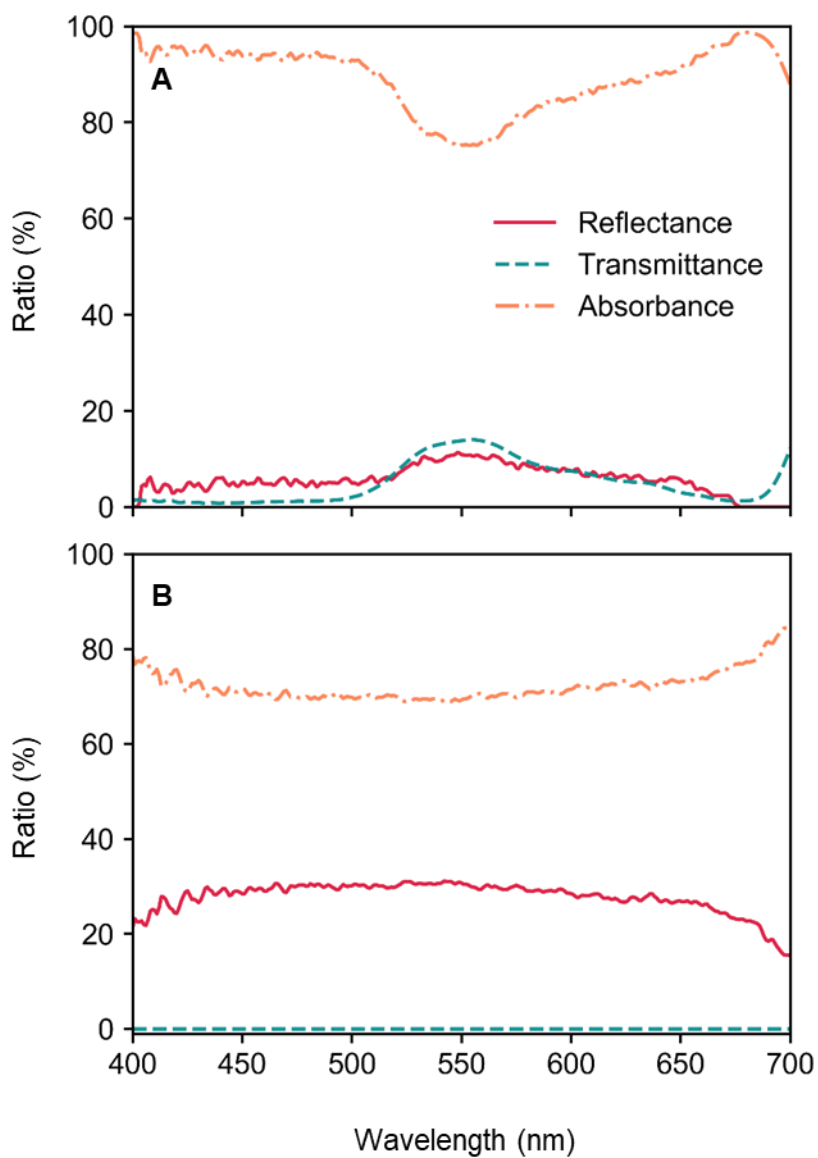
Appendix 1. Measured light reflectance, transmittance, and absorbance of tomato leaf (A) and greenhouse structure (B).

Appendix 2. Daily external diffuse irradiance ratio (%) of the ray-tracing evaluation date.